# Nanocantilevers made of bent silicon carbide nanowire-in-silicon oxide nanocones

Ming Lin and Kian Ping Loh[a)]
*Department of Chemistry, National University of Singapore, 3 Science Drive 3, Singapore 117543*

Chris Boothroyd
*Institute of Material Research and Engineering, 3 Research Link, Singapore 117602*

Anyan Du
*Institute of Microelectronics, Singapore*

(Received 2 August 2004; accepted 12 October 2004)

We report the plasma-assisted synthesis of nanocones on a nickel-coated silicon substrate using tetramethyl silane as the gas precursor. These nanocones consist of coaxially aligned, crystalline $\beta$-SiC nanowires surrounded by conical-shaped, amorphous silicon oxide precipitates. The propensity of the SiC wire to undergo changes in the growth axis directs the bending of the nanocones, giving rise to structures resembling nanocantilevers. The growth mechanism that controls the nanostructure formation is discussed. © *2004 American Institute of Physics*.
[DOI: 10.1063/1.1828601]

Controlling nanostructure formation is one of the key steps in nanofabrication and has been the focus of intensive research efforts. For example, creating an architectured assembly of dimensional nanostructures is essential for device integration in field-emission, sensor and multitip arrays for dip-pen lithography, photonic waveguides, etc.[1–3] There have been extensive research efforts on the synthesis and assembly of nanowires and nanotubes for such mechanical or electronic applications. However, there are relatively few systematic studies on ways to precisely engineer the shape and form of the components for functional nanoscale mechanical devices. For example, a conical structure offers substantially higher mechanical and thermal stability than a narrow cylinder. Structurally, nanocones can have nanometer-sized tips and micrometer-sized bases, rendering their manipulation easier than nanotubes. Nanocones are also mechanically stiffer and less prone to bending and thermal shock, making them ideal candidates for scanning probe tips, or as nanosyringes for quantum dot injection into biological cells. Zhang[4] reported the chemical vapor deposition (CVD) synthesis of tubular graphite cones consisting of annular rings of graphene planes concentric with a hollow interior. The conical structure is due to the progressively shorter terrace edges going from the inside to outside, arising from the sequential growth of shorter secondary layers on the outer layers as the central tube grows upward. Khrisnan[5] used arc discharge methods to synthesize geometrically precise, hollow nanocones that consisted of folded conical graphene planes. Vladmir[6] balanced the growth and etching effects of acetylene-ammonia mixtures to synthesize carbon nanocones made of cylindrical carbon nanofibers surrounded by carbon precipitates on the outside. All the nanocone[4–7] structures reported thus far are straight-growing, crystalline cones made of carbon. In this study, we report the plasma CVD synthesis of silicon carbide nanowire-in-silicon oxide nanocone and discuss the mechanism responsible for the bending of the nanocone.

Silicon wafers coated with 20 nm of nickel film were introduced into a commercial microwave plasma CVD system (AsTex). The gas phase composition was tetramethyl silane diluted in hydrogen. The nickel-coated Si(100) substrate was pretreated at 800 °C in a pure hydrogen plasma at a substrate bias of −150 V for 20 min prior to growth. Typical growth conditions employed pressures of 20 torr with the flow rate set at 10 standard-cubic-centimeter per minute (sccm) of tetramethyl silane and 100 sccm of hydrogen, substrate bias: +20 V, and a substrate temperature of 900 °C. At the end of the deposition, a blue film could be seen, which has been identified by infrared spectroscopy to consist of silicon oxycarbide phases.

Visualization of the surface deposits by scanning electron microscopy (SEM) reveals the growth of both straight and bent conical fibers with an overall length of several micrometers, as shown in Fig. 1. The substrate is covered also with amorphous, ball-like deposits of silicon oxycarbide

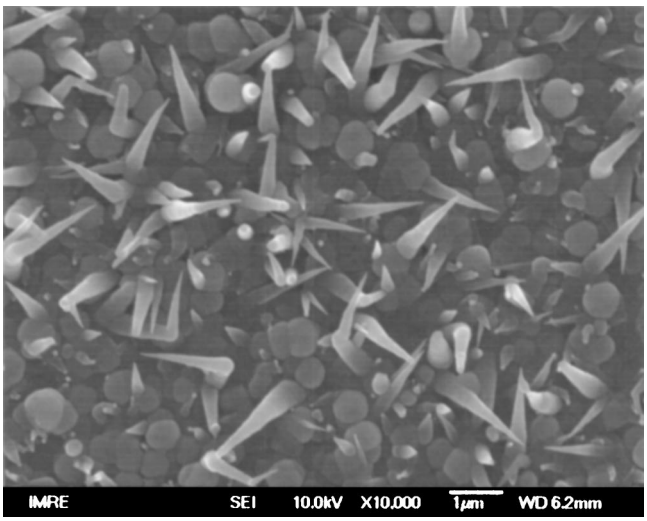


FIG. 1. SEM image of SiC-$SiO_x$ nanocones.

[a)]Author to whom correspondence should be addressed; electronic mail: chmlohkp@nus.edu.sg

 

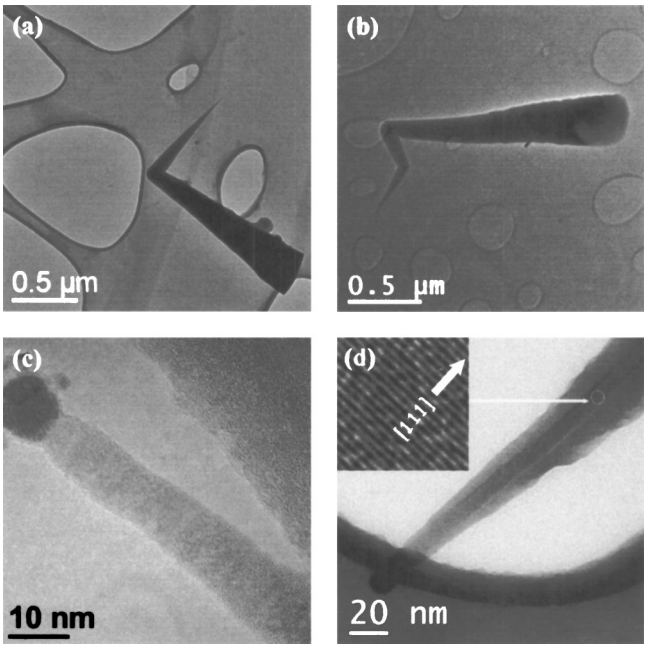


FIG. 2. (a) and (b) TEM images of bent nanocones; (c) a Ni catalytic particle at the tip of the cone; (d) HRTEM image shows that the inner nanowire is single-crystalline cubic SiC with the growth axis along the [111] direction.

about 0.5 μm in diameter. The base of the cone as seen in Fig. 1 is micrometer sized and is anchored in the micron-sized ball whilst the tip is nanometer sized. We believe that the microballs result from the encapsulation of individual nickel catalyst by a silicon oxycarbide coating. Low magnification TEM images in Figs. 2(a) and 2(b) show two typical bent nancones. Frequency analysis of the bending angles show that the majority of the angles are ~70° and 110°. A higher magnification view [Fig. 2(d)] reveals that the center of the cone has a coaxial crystalline wire of about ~5–10 nm diameter tipped by a catalyst particle [Fig. 2(c)]. The high-resolution image of this coaxial wire in Fig. 2(d) shows lattice fringe separations of 0.25 nm consistent with the cubic [111] $\beta$-SiC interplanar separations, whilst the outer coat is amorphous. The elemental composition has been verified by energy filtered electron energy loss imaging as shown in Fig. 3(a), the central wire is silicon carbide, whilst the outer conical coat is silicon oxide. The metal particle at the tip is nickel. Figure 3(b) shows that focusing the electron beam on the narrower regions of the cone (region *A*), where the wire is more prominent, produces an electron-energy-loss spectroscopy (EELS) spectrum which shows C *K* edge and Si *L*-edge, which are characteristic of SiC, whilst focusing on the thicker regions on the side of the cone (region *B*) produces and EELS spectrum with Si and O loss edges that are characteristic of silicon oxide.

Figure 4 shows the high-resolution TEM image of the junction of a bent nanowire changing its growth direction from [111] to [11$\bar{1}$]. At the turning juncture, we can see several thin strips of amorphous regions (denoted by a small white arrow) alternating with crystalline regions, and the growth is clearly disrupted in the forward direction by these amorphous regions. In the meantime, when the forward growth rate is slowed down, lateral growth in the [11$\bar{1}$] direction proceeds, and in the latter direction, there are fewer disruptions by the amorphous regions. Therefore, the devel-

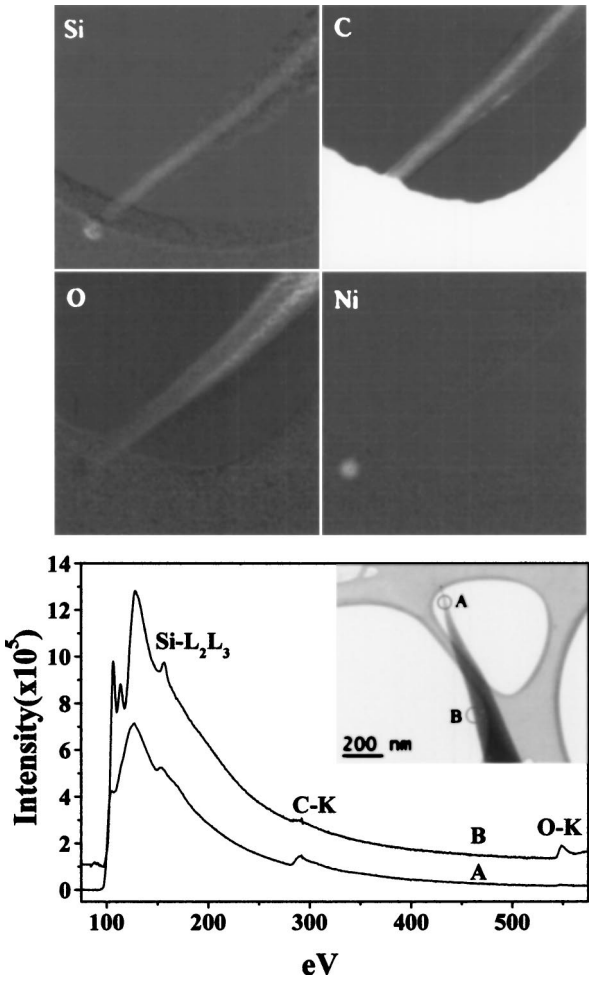


FIG. 3. (Top) EELS mapping of (a) Si, (b) C, (c) O, and (d) Ni in the nanocone. The elemental map clearly shows that the inner wire consists of SiC, and the outside is composed of $SiO_x$. (Bottom) EELS spectra recorded from SiC (region *A*) nanowire and sidewalls (region *B*).

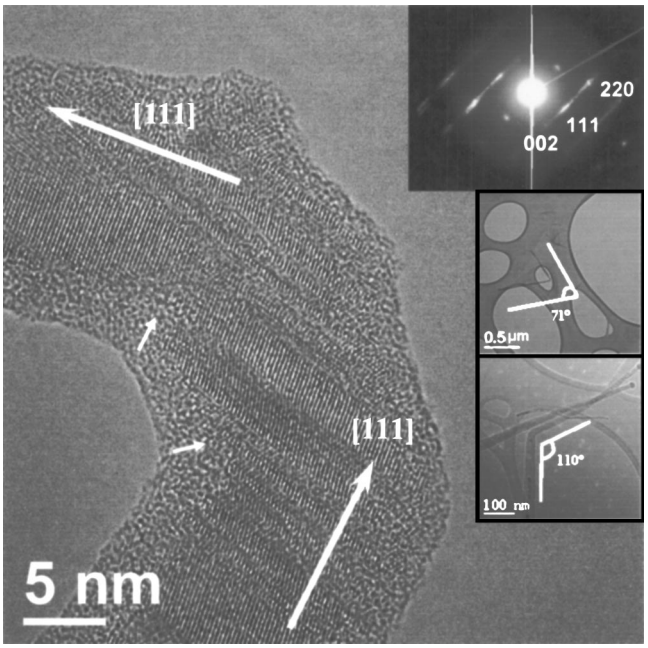


FIG. 4. HRTEM image of the junction of the bent SiC nanowire. The inset shows the diffraction pattern of this area, the other two images show two typical SiC nanowires with bending angles of 70° and 110°.

opments of multiple defective regions in one direction slow down the rate of crystalline growth in that direction, whilst encouraging branching growth in another direction.

The presence of a nickel catalyst at the tip of the SiC nanowire suggests tip-catalyzed growth following the classic vapor-liquid-solid mechanism.[8] The presence of an outer amorphous $SiO_x$ coat indicates that lateral growth of amorphous $SiO_x$ occurred on the SiC wire template simultaneously. Unlike carbon nanotube, the stacking of cubic crystal planes to form a wire in the case of $\beta$-SiC creates a high density of reactive edge sites on the periphery of the wire, these are inevitably oxidized by oxygen to form $SiO_x$.[9–11] Depending on the rate of the lateral growth of $SiO_x$ relative to the vertical growth of the SiC wire, either a coaxially aligned nanowire or wire-in-cone structure results. The lateral growth of the $SiO_x$ results from the rapid precipitation of gaseous $SiO_x$ species in the plasma on the reactive sidewalls. Placing the sample away from the plasma ball reduces the rate of $SiO_x$ precipitation, and longitudinal nanofibers are obtained instead, thus evidencing that it is the rate of oxide growth that determines the morphology. We observe that the $\beta$-SiC nanofiber has an intrinsic propensity to undergo changes in the growth axis due to the ease of generating twin boundaries and stacking faults when stacking cubic planes anisotropically.[9–11] The inset in Fig. 4 shows TEM images of silicon carbide nanofibers grown on samples placed farther away from the plasma ball. At regions away from the intense plasma zone, the precipitation rate of $SiO_x$ is slower, and only $\beta$-SiC nanowire is obtained. Several bent nanowires can be seen. The bending angles of 70 and 110 °C in the nanowires are defined by the interplanar angles between [111] and $[11\bar{1}]$ planes. The internal microstructure of consists of a $SiO_2$-sheathed, coaxially structured $\beta$-SiC nanowire.

Previous studies of $SiO_2$-ensheathed SiC nanowires revealed that the growth axis of the latter changed frequently between the $\{x11\}$ family planes ($x=1$, 2, or 3) in the course of growth, resulting in a zigzag coursing along the wire,[9] however, nanocones or nanowires with bending angles $>50$ °C had not been reported. The nanowire grows along the [111] direction when there is a high density of twins on the sidewalls. If the sidewalls are defect free, then the growth direction has to be maintained in the [211] direction instead. A detailed look at the $\beta$-SiC nanowire produced here reveals that most of the nanowires are growing in the [111] direction with a high density of twin defects at the sides, giving rise readily to change in growth axis in the $[11\bar{1}]$ direction. At the turning juncture, it consists of stacking faults and is interspersed with amorphous segments. There was no intentional introduction of oxygen into the growth environment, but the trace oxygen in the growth environment contributed a low concentration of directional oxygen ions normal to the plane of the substrate. This can have a modulating effect on the stacking of the crystal planes by influencing a higher rate of oxide growth on crystal faces that have a high density of stacking defects, or dangling bonds.

Since the SiC wire acts as a template for the lateral growth of $SiO_x$, the turning SiC wire causes a similar turn in the conical $SiO_x$ deposit around it, resulting in the growth of a bent nanocone. The amorphous nature of the $SiO_x$ deposit allows the smooth merging of interfaces between the segments of the bent cones that would otherwise be difficult for crystalline systems. Branching growth of the nanocones from a connected base can also be explained by the merging of the $SiO_x$ deposits between two adjacent SiC nanowires. The growth of the bent nanocone is a phenomenon restricted to the unique material combination of a cubic phase wire and an amorphous oxide sheath. Thus far, there have been no reports of bent nanocones for the graphitic system, because the growth mechanism precludes the sharp angular bending of crystalline graphene sheets in the *c* axis. The amorphous phase has no such restrictions and remarkable branching and merging between interfaces of silicon oxide nanowires to form branching networks have been recently reported.[12,13]

The SiC wire-in-silicon oxide nanocones are potentially useful for structural applications due to its mechanical strength. For example, the catalyst at the SiC nanowire tip can be removed to expose a short section of SiC nanowire tip which has its stem encapsulated by a mechanically stiff $SiO_x$ coat. The bent nanocone resembles a nanocantilever and can be used as an atomic force microscope probe with the SiC nanowire tip. Engineering straight SiC wire-in-silicon oxide nanocones, however, is difficult since it is not known whether the initial impetus for a change in growth direction of the SiC nanowire is purely random, i.e., plasma process fluctuations, entropy driven, etc. It is possible that stacking defects were induced by oxygen ions in the plasma, because a much higher density of bent nanowires was observed in this work compared to previous studies. One possibility to direct the growth of the nanocone may be using templates with nanosized channels to externally constrict the bending angles.

In summary, we have synthesized a $\beta$-SiC nanowire-in-$SiO_x$ nanocone structure using CVD. Our results suggest that cubic phase nanowires are readily ensheathed by an amorphous oxide in plasma CVD. A change in the growth direction of this wire from [111] to $[11\bar{1}]$, due to stacking faults and twinning defects common to nanowires of the cubic phase, guides the growth of a bent nanocone.

K.P.L. wishes to acknowledge the support of NUSNNI and NUS Academic Grant (No. R-143-000-162-112) for the support of this research.

[1] R. D. Piner, J. Zhu, F. Xu, S. H. Hong, and C. A. Mirkin, Science **283**, 661 (1999).
[2] K. B. K. Teo, M. Chhowalla, G. A. J. Amaratunga, W. I. Milne, G. Pirio, P. Legagneux, F. Wyczisk, D. Pribat, and D. G. Hasko, Appl. Phys. Lett. **80**, 2011 (2002).
[3] L. E. Greene, M. Law, J. Goldberger, F. Kim, J. C. Johnson, Y. F. Zhang, R. J. Saykelly, and P. D. Yang, Angew. Chem., Int. Ed. **42**, 3031 (2003).
[4] G. Y. Zhang, X. Jiang, and E. G. Wang, Science **300**, 472 (2003).
[5] A. Krishnan, E. Dujardin, M. M. J. Treacy, J. Hugdahl, S. Lynum, and T. W. Ebbesen, Nature (London) **388**, 451 (1997).
[6] V. I. Merkulov, M. A. Guillorn, D. H. Lowndes, M. L. Simpson, and E. Voelkl, Appl. Phys. Lett. **79**, 1178 (2001).
[7] R. C. Mani, X. Li, M. K. Sunkara, and K. Rajan, Nano Lett. **3**, 671 (2003).
[8] R. S. Wagner, and W. C. Ellis, Appl. Phys. Lett. **4**, 39 (1964).
[9] Z. L. Wang, Z. R. Dai, R. P. Gao, Z. G. Bai, and J. L. Gole, Appl. Phys. Lett. **77**, 3349 (2000).
[10] Y. J. Xing, Q. L. Hang, H. F. Yan, H. Y. Pan, J. Xu, D. P. Yu, Z. H. Xi, Z. Q. Xue, and S. Q. Feng, Chem. Phys. Lett. **345**, 29 (2001).
[11] Y. Q. Zhu, W. B. Hu, W. K. Hsu, M. Terrones, N. Grobert, J. P. Hare, H. W. Kroto, D. R. M. Walton, and H. Terrones, J. Mater. Chem. **9**, 3173 (1999).
[12] Y. H. Gao, Y. Bando, K. Kurashima, and T. Sato, J. Mater. Sci. **37**, 2023 (2002).
[13] H. J. Li, Z. J. Li, A. L. Meng, K. Z. Li, X. N. Zhang, and Y. P. Xu, J. Alloys Compd. **352**, 279 (2003).